Journal of Alloys and Compounds 509 (2011) 3006–3012

Contents lists available at ScienceDirect

Journal of Alloys and Compounds

journal homepage: www.elsevier.com/locate/jallcom

Microstructures evolution and phase transformation behaviors of Ni-rich TiNi shape memory alloys after equal channel angular extrusion

Xiaoning Zhang[a], Jie Song[a], Chenglong Huang[b], Baoyu Xia[a], Bin Chen[a], Xiaogang Sun[a], Chaoying Xie[a,*]

[a] State Key Lab of Metal Matrix Composites, School of Materials Science and Engineering, Shanghai Jiao Tong University, Shanghai 200240, China
[b] Department of Orthopaedics, Sixth People's Hospital Affiliated to Shanghai Jiao Tong University, Shanghai 200233, China

ARTICLE INFO

Article history:
Received 8 September 2010
Received in revised form 5 November 2010
Accepted 10 November 2010
Available online 3 December 2010

Keywords:
TiNi shape memory alloys
Equal channel angular extrusion (ECAE)
Microstructure evolution
Phase transitions

ABSTRACT

Ni-rich TiNi shape memory alloys were subjected to the effect of equal channel angular extrusion (ECAE) processes at 773 K by Bc path. The effects of ECAE processes on microstructures evolution and phase transformation behaviors were investigated. The initial 60–80 μm equiaxed coarse grains of samples were elongated along the shearing force direction of ECAE and refined to 300–400 nm after eight passes ECAE. The R phase transformation of Ni-rich TiNi shape memory alloys was stimulated by ECAE processes within a larger temperature range. The martensite transformation peak temperature (Mp) dropped in previous 1–3 ECAE treatments, but the dropped Mp increased gradually with the increase of ECAE processes. Ti_3Ni_4 phase was observed in the regions with high density of dislocations after ECAE treatment. Reasons for microstructures evolution and phase transformation changes were also discussed.

1. Introduction

Ultra-fine grained materials, which are widely applied in many fields for their higher mechanical performance, have an average grain size smaller than 1 μm. In the last decade, some different severe plastic deformation (SPD) techniques were developed extensively for the effective production of these metallic materials [1]. As one of the SPD methods, the equal channel angular extrusion (ECAE) technique was first introduced by Segal and his colleagues in 1970s and 1980s [2,3]. The method had been applied in the production of various ultrafine grain materials successfully, such as TiNi alloys [4–12], TiAl alloys [13], Ti [14–16], Mg, Al and Cu alloys [17–25] and some interesting results were obtained [26–29].

The TiNi system has been of extensive application prospects due to the unique shape memory effect (SME) and the pseudoelasticity (PE) which occurs mostly in the near equiatomic TiNi alloys [30,31]. They are applied widely in the world for superb properties such as the biocompatibility, the maximum recoverable strain and stress, and excellent corrosion resistance. The unusual SME and PE properties originate from the so-called thermoelastic martensite transformation [32].

Although martensite transformation behaviors are important characters for Ni-rich TiNi shape memory alloys, its phase transformation behaviors after ECAE treatment are seldom studied systematically. Li has investigated on the microstructures evolution and phase transformation behaviors of Ti–50.3 at.% Ni alloy during two passes ECAE at 1123 K and 1023 K [33,34]. Because the accumulated deformation was not enough in relatively few ECAE treatments and the temperature of ECAE processes was comparatively higher, the submicron grains after ECAE treatment were still large in Li's studies. It was insufficient to understand the two aspects of TiNi alloys after ECAE treatment. Fan also researched the R phase transformation of multiple ECAE treatments [7,8]. However, the solution treatment conditions of Ni-rich TiNi alloy in this study are different with those of in the previous investigation. Even more important, Ti_3Ni_4 precipitates after ECAE processes were not found in the past work. This study focuses on the microstructures evolution and the phase transformation behaviors of Ni-rich TiNi alloys after multiple ECAE treatments at warm temperature 773 K by Bc path. The initial equiaxed coarse grains can be refined to submicron grains after the ECAE treatments. A special R phase transformation behavior and Ti_3Ni_4 precipitation after ECAE treatment are systematically analyzed by DSC and TEM, respectively. This investigation will be helpful for better understanding the phase transformation behaviors of TiNi SMAs.

2. Experimental

The initially hot forged Ni-rich Ti–50.9 at.% Ni alloy (nominal composition) rods were annealed at 1123 K for 1 h, and then cooled into water directly (solution treatment). The Ni-rich Ti–50.9 at.% Ni alloy rods were cut into the billets with the 10 mm × 10 mm × 140 mm dimensions. The inner contact angle (Φ) and the arc of curvature (Ψ) at the outer point of contact between channels of the die were both 90°, as shown in Fig. 1. It was well known that an effective strain of ~1 produced in the single pass of the ECAE treatment.

* Corresponding author. Tel.: +86 21 54742608.
E-mail addresses: zxn100@gmail.com (X. Zhang), cyxie@sjtu.edu.cn (C. Xie).

0925-8388/$ – see front matter © 2010 Elsevier B.V. All rights reserved.
doi:10.1016/j.jallcom.2010.11.189

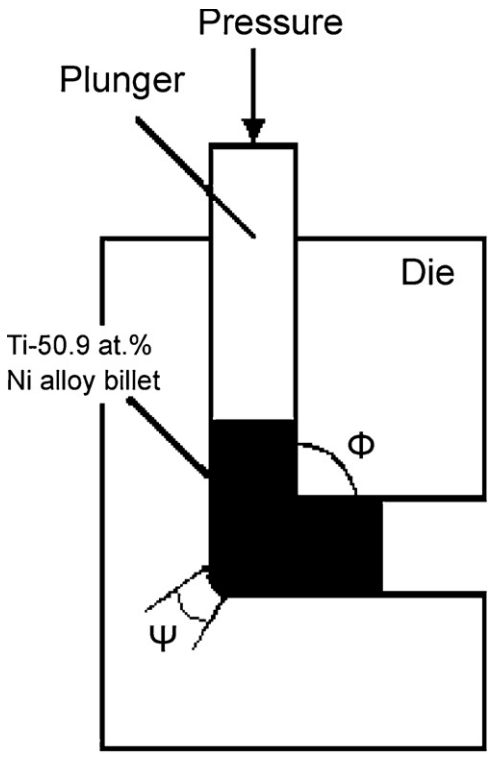

Fig. 1. Schematic illustration of the ECAE facility in the experiment.

ECAE processes were conducted at 773 K via Bc path between each pass (the billet was rotated by 90° either clockwise or counter-clockwise). During every ECAE process, the billet was preheated at 773 K for 20 min. It would be better for ECAE treatment and coating with graphitic lubricant to minimize friction, and thus eliminate the sticking between the specimens and the die during the extrusion processes.

For the metallographic observations, differential scanning calorimeter (DSC) measurements and TEM observations, the samples were cut from the longitudinal plane of deformed billets that parallel to the extrusion direction of ECAE. Specimens for optical texture examination were prepared by metallographic polishing and etched by a mixture of HF, HNO_3 and H_2O with a volume ratio of 1:3:10. The experiments were performed with Zeiss optical microscope. DSC measurements were carried out to analyze the phase transformation behaviors with the Diamond DSC machine (PerkinElmer Company of American). The range of DSC test temperatures was in 183–373 K. The heating and cooling rate was 10 K/min. Samples of TEM observation were prepared by twin jet electro-polishing at 243 K and with manipulation voltage of 30 V. The twin jet mixture solution was H_2SO_4 and CH_3OH with a volume ratio of 1:4. TEM experiments were conducted on the JEM-2100F (JEOL) with an accelerating voltage of 200 kV.

3. Results and discussion

3.1. Evolution of the microstructures of Ti–50.9 at.% Ni alloy

3.1.1. Optical microstructures observation

Microstructures of Ti–50.9 at.% Ni alloy with different ECAE processes are shown in Fig. 2. It was revealed that the size of these equiaxed coarse grains were approximately 60–80 μm after solution treatment, as shown in Fig. 2a. After the first ECAE treatment, these equiaxed grains were deformed severely and elongated along the shearing force direction of ECAE. Moreover, some shear bands were formed and could be observed under the optical microscope, as shown in Fig. 2b. Compared with the first ECAE treatment, the second ECAE treatment resulted in denser shear bands. These grains were partially broken down under the shearing force. Paralleled to the shear direction, these grains were elongated dramatically. It could be identified clearly that the average size of the grains decreased notably, as shown in Fig. 2c.

The microstructure of the sample with the fourth ECAE treatment is shown in Fig. 2d. These submicron grains were refined more largely, and it is difficult to observe these submicron grains and grain boundaries under the optical microscope. After the sixth and eighth ECAE treatment, these submicron grains and grain boundaries were elongated and broken deeply once again along the direction of ECAE. Although some fine submicron grains were lengthened along the shearing force direction, finer equiaxed and ultrafine grains in the interior were formed, as shown in Fig. 2e and f, respectively.

3.1.2. TEM observation

The microstructures evolution of the different passes ECAE treatment was further observed by TEM observation. Typical TEM observations of Ti–50.9 at% Ni alloy with distinct ECAE processes are shown in Fig. 3. The initial equiaxed coarse grains were elongated along the shearing force direction. From the top to bottom surfaces of the sample, many coarse grains were guided essentially parallel long blocks with a width of ~0.5 μm after the first ECAE treatment. Moreover, many regions with high density of dislocations were distributed in the elongated grains, as shown in Fig. 3a. The microstructure of the fourth and eighth passes ECAE is shown in Fig. 3b and c, respectively. These elongated grains after the first ECAE treatment were replaced mostly by an array of equiaxed submicron grains with an average grain size of ~600 nm after the fourth ECAE treatment, and further were refined to 300–400 nm after the eighth ECAE treatment. It was suggested that a higher stress is required in the stress-induced martensite transformation (SIM) for an ultrafine grain size [9]. In martensite phase transformations of ultrafine grain structured materials, geometrical constraints such as the grain boundaries with high density and the ultrafine grains could contribute to the transformation barrier, and thus cause the change of the martensite transformation path [35]. Selected area electron diffraction (SAED) was conducted to study the detail information of the deformed samples, as shown in the inset patterns of Fig. 3b and c, respectively. These inset SAED patterns revealed important differences between Fig. 3b and c. Inspection of Fig. 3b SAED pattern showed that the diffracted beams tend to be scattered around rings, so that some of the submicron grain boundaries now have certain misorientations with high angles. Fig. 3c SAED pattern demonstrates conclusively that the submicron grain boundaries are more in high angles of misorientation. It appears that the microstructure is now fairly similar to a well solution-treatment condition except only that the submicron grains size of the material is extremely small, the average submicron grains size of 300–400 nm. These mean that the submicron grains size of the eighth ECAE treatment is much smaller and well-distributed than that of the fourth.

In every ECAE process, the billet was preheated at 773 K for 20 min. The recrystallization phenomenon might be caused at the higher temperature preheating processes. After the first pass ECAE, static recrystallization occurred during heating at 1023 K for 20 min before the second ECAE. However, no recrystallization occurred at a relatively lower temperature (773 K or 873 K) even though with a longer annealing time for 2 h after the second passes ECAE [34]. The recrystallization phenomenon might be mainly decided by the preheating temperature rather than preheating time. Fan had done some studies on the recrystallization of ECAE treatment [7]. For the first pass ECAE specimens, some tiny recrystallized grains appeared at an annealing temperature 913 K with 20 min annealing time, while recrystallization temperature decreased to 873 K for 20 min after the eighth passes [7]. It was reported that ECAE processes may accumulate some energy for subsequent recrystallization [36]. More energy can be accumulated obviously in the eighth ECAE treatment than the first ECAE treatment, which reasonably results in the decrease of the recrystallization temperature.

No matter the first or eighth ECAE process, recrystallized grains would not appear during the preheating treatment at 773 K for 20 min, or even for a much longer heating time [7]. Based on these

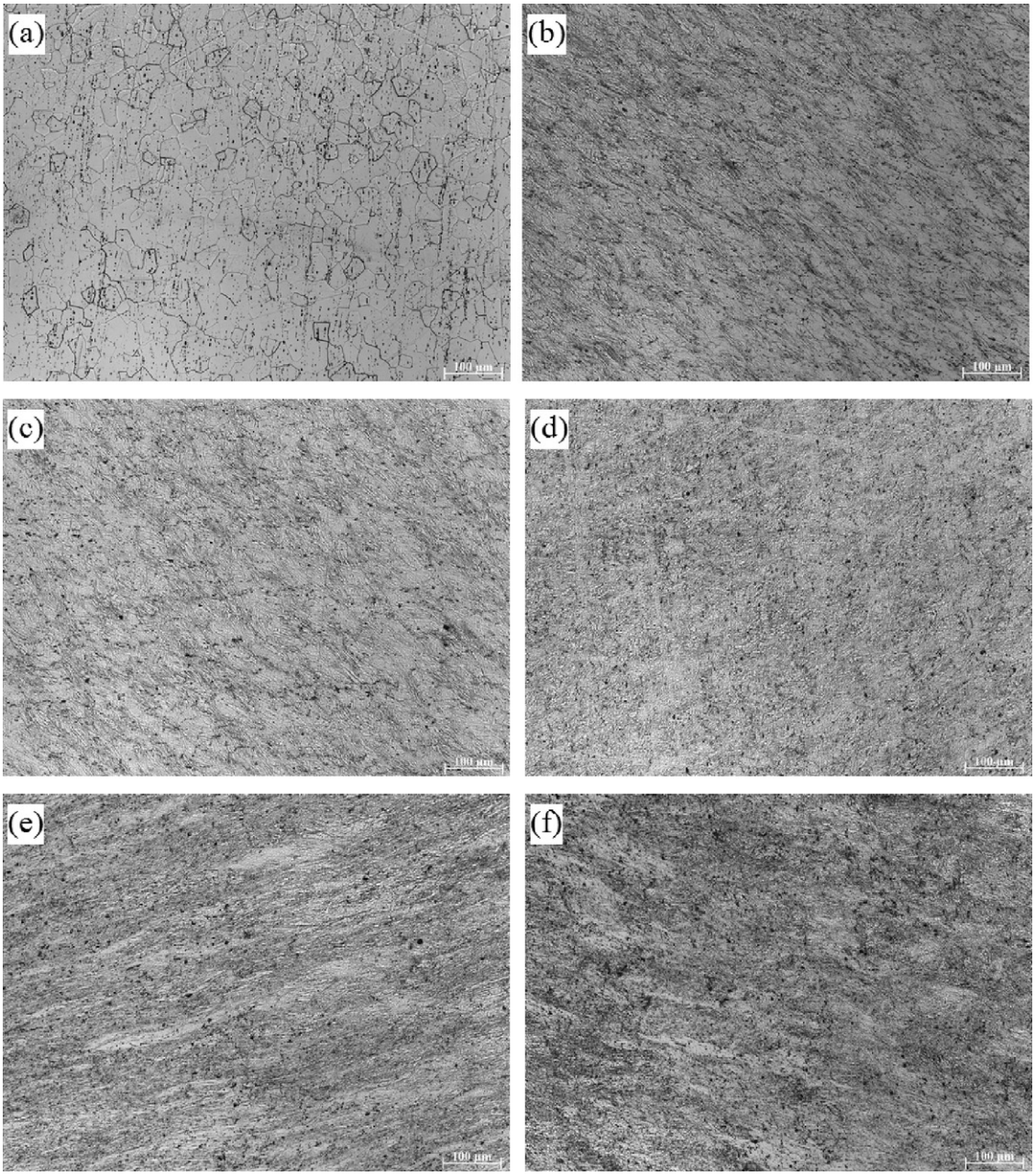

Fig. 2. Microstructures evolution of Ti–50.9 at.% Ni alloy with different ECAE processes at 773 K by Bc path: (a) solution treatment; (b) first pass; (c) second passes; (d) fourth passes; (e) sixth passes; (f) eighth passes.

Table 1
Phase transformation temperature of Ti–50.9 at.% Ni alloy before and after ECAE processes.

Procedures	Temperature (°C)					
	Ms	Mp	Mf	As	Ap	Af
Solution treatment	−12.54	−31.66	−49.90	−19.78	−8.11	12.67
First pass ECAE	–	–	–	−9.53	−0.81	17.44
Second passes ECAE	−50.35	−59.85	−78.33	−10.43	1.73	18.66
Third passes ECAE	−49.26	−66.96	−82.86	−6.34	4.49	20.01
Fourth passes ECAE	−49.55	−60.69	−80.58	−16.93	0.61	14.03
Fifth passes ECAE	−41.95	−54.36	−79.95	−3.76	8.63	17.01
Sixth passes ECAE	−47.14	−56.09	−81.03	4.53	10.50	15.03
Seventh passes ECAE	−33.08	−52.18	−85.14	1.54	13.07	19.45
Eighth passes ECAE	−41.85	−49.70	−68.93	3.36	14.18	19.71

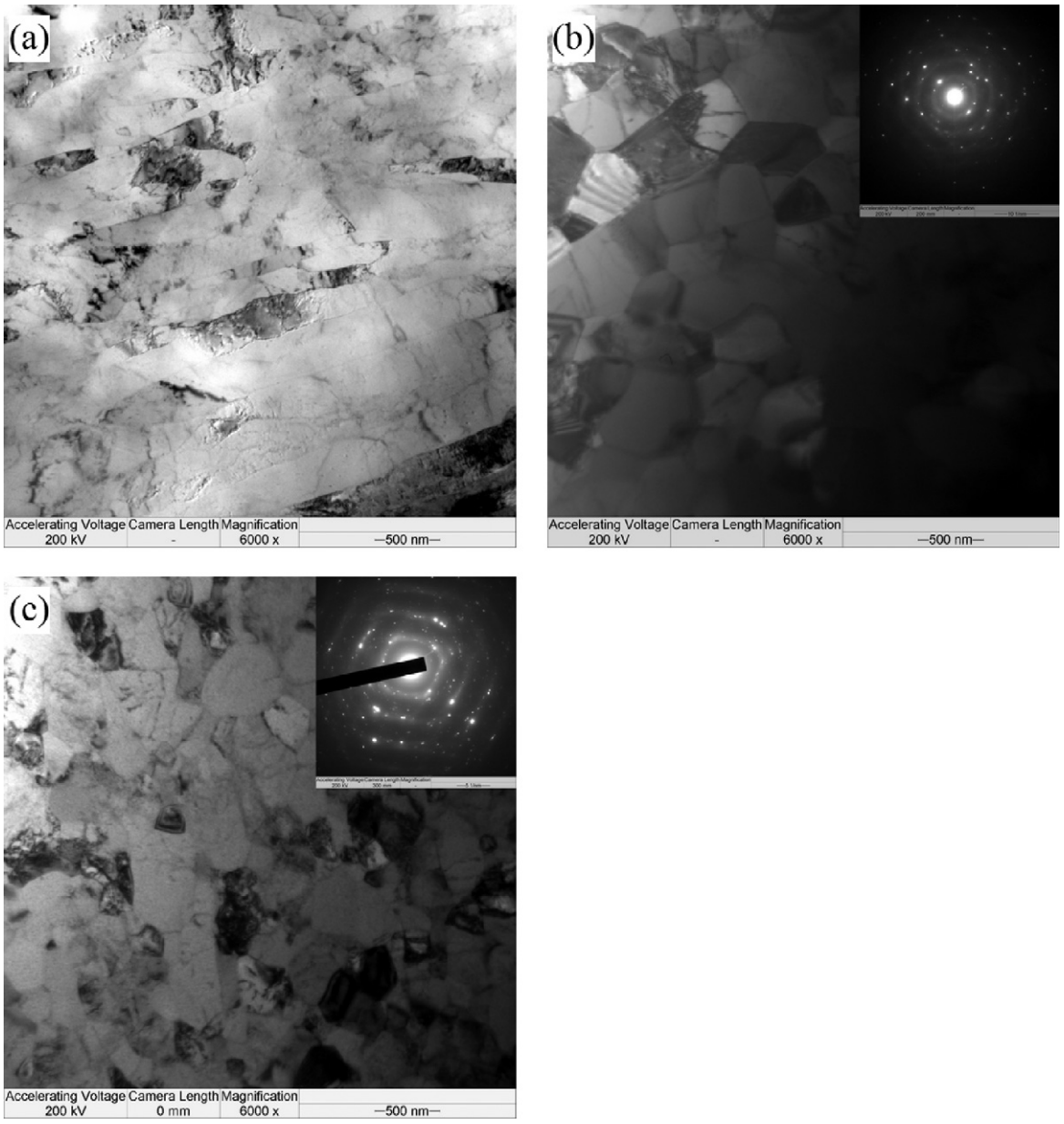

Fig. 3. Microstructures and SAED patterns of Ti–50.9 at.% Ni alloy after different ECAE processes at 773 K by Bc path: (a) first pass; (b) fourth passes; (c) eight passes.

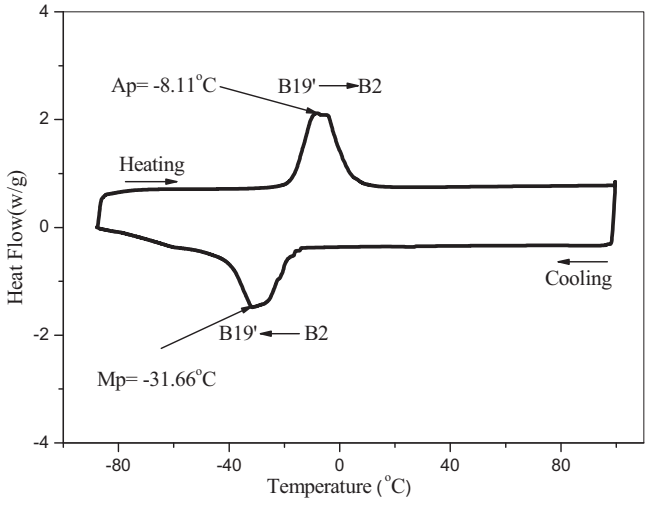

Fig. 4. DSC curves of solution treatment Ti–50.9 at.% Ni alloy.

experiments, it can be confirmed that the recrystallization temperature for ECAE process is higher than 773 K (the experiment temperature). Therefore, there was no recrystallization in the preheating process of every ECAE treatment.

3.2. Effects of ECAE processes on transformation behaviors

3.2.1. DSC analysis

There are three transformations related to these special functions upon cooling in near equiatomic TiNi alloys, the B2 → B19′, B2 → R and R → B19′ [37]. The B2 → R transformation is also martensite transformation with smaller lattice deformation and temperature hysteresis. It is different with the martensite transformation B2 → B19′. Owing to these unique characteristics, TiNi alloys with B2 → R transformation would be applied in the actuators and sensors potentially [37,38].

The phase transformation behaviors of Ti–50.9 at.% Ni alloy solution treated are shown in Fig. 4. When the specimen was cooled down from 373 K to 183 K, only an exothermic peak was observed that corresponded to phase transformation from the B2 parent

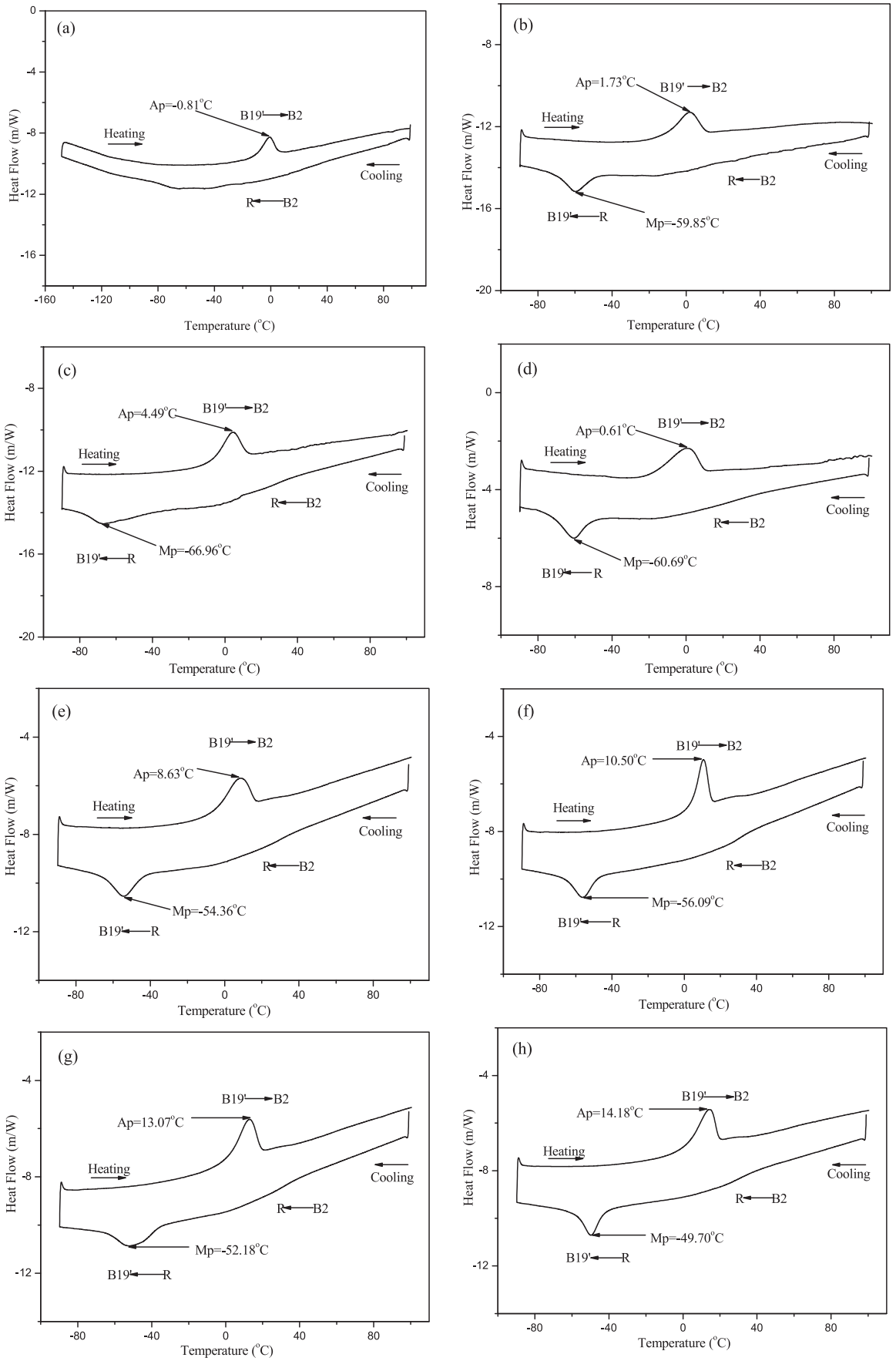

Fig. 5. DSC curves of Ti–50.9 at.% Ni alloy after ECAE processes at 773 K by Bc path: (a) first pass; (b) second passes; (c) third passes; (d) fourth passes; (e) fifth passes; (f) sixth passes; (g) seventh passes; (h) eighth passes.

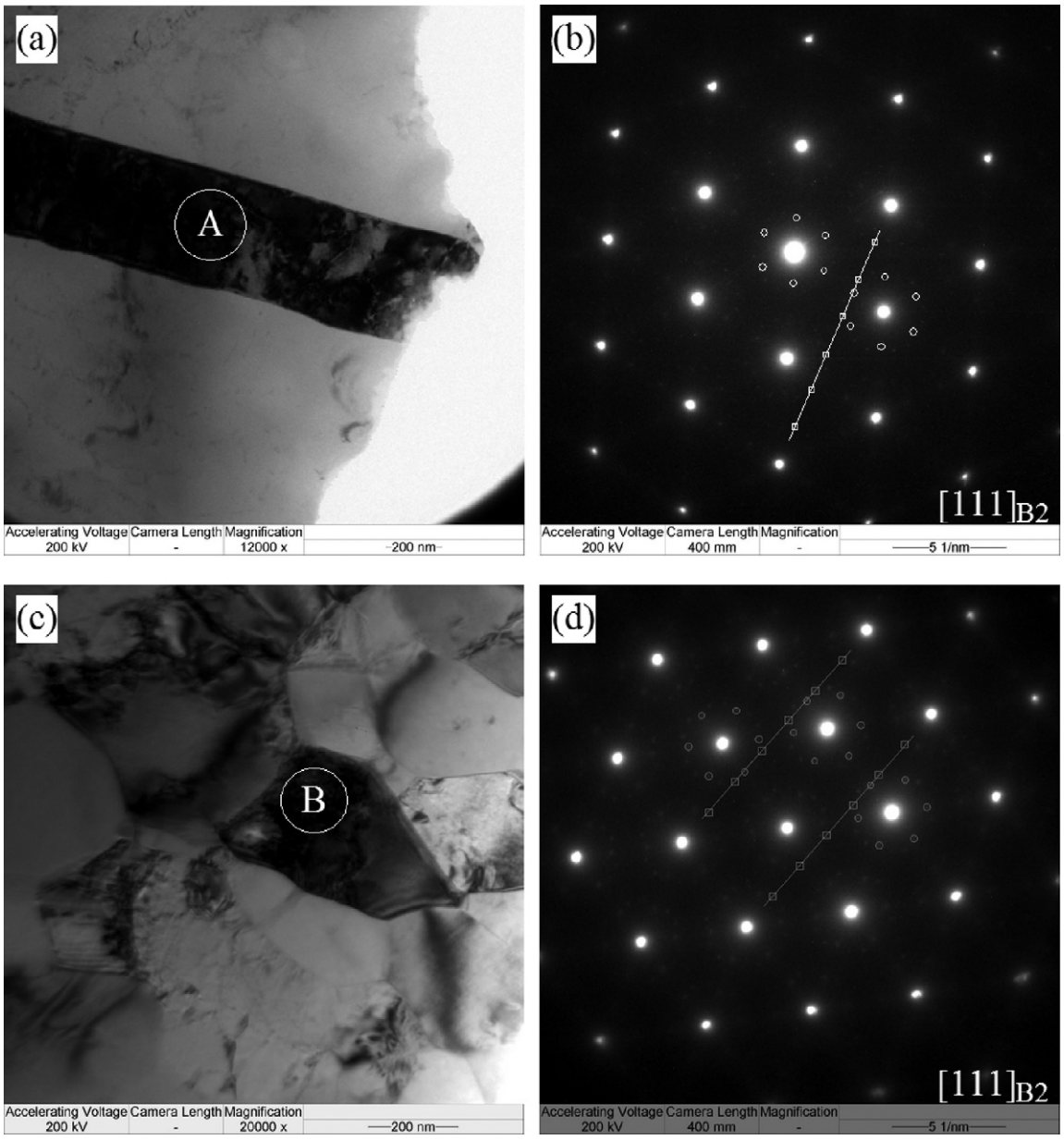

Fig. 6. Microstructures and SAED patterns of Ti–50.9 at.% Ni alloy after the first pass and the eighth passes ECAE at 773 K by Bc path: (a) bright field images of first pass; (b) SAED pattern of A regain of (a); (c) bright field images of eighth passes; (d) SAED pattern of B regain of (c).

phase to the B19′ martensite phase. When the specimen was heated up from 183 K to 373 K, the endothermic peak found that corresponded to the B19′ → B2 reverse martensite phase transformation.

The phase transformation behavior of Ti–50.9 at.% Ni alloy after ECAE treatment at 773 K is shown in Fig. 5. After the first pass ECAE, the exothermic peak was too low to be observed when the specimen was cooled even in the 123 K, as shown in Fig. 5a.

Compared with solution treatment Ti–50.9 at.% Ni alloy phase transformation, the martensite transformation peak temperature (Mp) has dropped a lot from the second to the eighth passes ECAE, as shown in Fig. 5b–h. Two exothermic peaks appeared when the specimen cooled down from 373 K. It corresponded to the phase transformation from B2 parent phase to the R phase, and then from R phase to B19′ martensite phase [39]. The B2 → R phase transformation can be seen on the DSC curves, but it occurred in a wider temperature extent and these curves were broad and smooth.

At the initial stage, the Mp decreased gradually as the ECAE passes increased. However, the Mp increased after subsequently ECAE treatment course which may be resulted from the precipitation of Ti_3Ni_4. As well known, the precipitation of Ti_3Ni_4 decreased the Ni content in the matrix which could be resulted in the increase of the temperature of the martensite phase transformation after the ECAE treatment [40]. The Ti_3Ni_4 particles have an important effect on the martensite transformations. The dispersed Ti_3Ni_4 particles would serve as the nucleation sites of the R phase transformation. Because the crystal lattices are similar; the growths of Ti_3Ni_4 in the B2 matrix favor a B2 → R transformation. By contrast, the B2 → B19′ transformation is hampered, because these dispersed particles presented in the matrix would require more additional energy expenditure owing to a higher elastic energy of the system [41]. On the heating curves of DSC for all ECAE samples from the first to the eighth pass, only one endothermic peak was observed, which revealed that the reverse R phase transformation and the reverse martensite phase transformation overlapped together [42]. Furthermore, the austenite peak temperature (Ap) increased gradually as the ECAE treatments increased. Table 1 shows the phase trans-

formation temperature of the martensite and austenite start (Ms, As), peak (Mp, Ap) and finish temperature (Mf, Af) of Ti–50.9 at.% Ni alloy with the solution treatment and ECAE processes.

3.2.2. TEM and SAED analyses

The more detail information of Ti_3Ni_4 phase was studied by TEM (Fig. 6a and c) and selected area electron diffraction pattern (SAED, Fig. 6b and d). The magnified microstructures of the first ECAE clearly demonstrated a single elongated grain, as shown in Fig. 6a. In Fig. 6b, the SAED pattern is corresponded to the selected region (marked A in Fig. 6a). It was noticed that $1/3\langle 1\,1\,0\rangle_{B2}$ super-lattice spots marked with some white circles, and accompanying with $1/7\langle 1\,2\,3\rangle_{B2}$ super-lattice spots marked with some white squares bunched by a white line, could be observed in the SEAD pattern of the first ECAE treatment.

Compared with the first ECAE treatment, the sample obtained after the eighth ECAE has the finer submicron grains with an average grain size of about 300–400 nm. Most submicron grains exhibited equiaxed submicron grains morphology and the submicron grain boundaries increased obviously, as shown in Fig. 6c. Fig. 6d is the SAED pattern which corresponded to the selected region (marked B in Fig. 6c). The $1/3\langle 1\,1\,0\rangle_{B2}$ and the $1/7\langle 1\,2\,3\rangle_{B2}$ super-lattice spots of the SAED pattern in Fig. 6d remain the same as Fig. 6b, which revealed that there was R phase transformation formed in both EACE processes [43]. However, the characterized $1/7\langle 1\,2\,3\rangle_{B2}$ super-lattice spots of Ti_3Ni_4 phase (some white squares bunched by a white line) are observed in Fig. 6b and d, which suggested Ti_3Ni_4 precipitated in the regains with high density of dislocations of the first pass and the eighth passes ECAE treatment samples.

Obviously, the B2 → R phase transformation may result from ECAE processes, in which these coarse and equiaxed grains were refined dramatically. The grain boundary fractions increased largely, and a lot of defects such as dislocations were introduced into the grains interior and boundaries. Under the action of extrusion force in the ECAE process, many dislocations were slipped and piled up around grain boundaries [44]. These excessive grain boundaries and dislocations in the grain interior and exterior probably stimulated the B2 → R phase transformation and suppressed the R → B19′ phase transformation. At the same time, the Mp temperature decreased, which resulted from all the defects and dislocations formed during ECAE processes. Another factor may be that local stress fields were created by the non-uniform microstructures resulted from the ECAE process, and thus induced the B2 → R phase transformation [45].

As a consequence, the martensite phase transformation occurred in two steps: B2 → R and R → B19′ during the cooling process. And the Mp temperature after ECAE treatments decreased compared with the solution treatment. The further details of the B2 → R and R → B19′ phase transformation in Ni-rich TiNi alloys after ECAE treatments will be investigated and discussed in future.

4. Conclusions

Ni-rich Ti–50.9 at.% Ni alloy after multiple ECAE treatments was studied, and the following conclusions can be drawn from the present experimental results:

1. Ni-rich Ti–50.9 at.% Ni alloy was subjected to the effect of ECAE processes at 773 K by Bc path. The initially coarse and equiaxed 60–80um grains were refined dramatically to 300–400 nm submicron grains after the eighth passes ECAE.
2. The billet was preheated at 773 K for 20 min for graphitic lubricant coating better and ECAE treatment. And recrystallized grains of billets would not appear in the preheating process.
3. After ECAE processes, the martensitic phase transformation underwent in two steps: B2 → R → B19′. Compared with the solution treated, the Mp of ECAE treatment decreased a lot. The Mp decreased in previous 1–3 ECAE treatment, but increased gradually with more ECAE processes.
4. Ti_3Ni_4 phase was observed in the regions with high density of the dislocation of ECAE treatment Ni-rich Ti–50.9 at.% Ni alloy.

Acknowledgement

Our research was supported by National Science Fund of China (Grant No. A50671067).

References

[1] K.S. Raju, M.G. Krishna, K.A. Padmanabhan, K. Muraleedharan, N.P. Gurao, G. Wilde, Mater. Sci. Eng. A 491 (2008) 1–7.
[2] V.M. Segal, V.I. Reznikov, F.E. Drobyshevskii, V.I. Kopylov, Izv. AN SSSR. Metally. No. 1 (1981) 115–123 (in Russian).
[3] V. M. Segal, USSR Patent No. 575,892 (1977).
[4] J. Ma, I. Karaman, H.J. Maier, Y.I. Chumlyakov, Acta Mater. 58 (2010) 2216–2224.
[5] B. Kockar, K.C. Atli, J. Ma, M. Haouaoui, I. Karaman, M. Nagasako, R. Kainuma, Acta Mater. 58 (2010) 6411–6420.
[6] K.C. Atli, I. Karaman, R.D. Noebe, H.J. Maier, Scripta Mater. 64 (2011) 315–318.
[7] Z. Fan, C. Xie, Adv. Mater. Res. 26–28 (2007) 385–388.
[8] Z. Fan, C. Xie, Mater. Sci. Forum 561–565 (2007) 2313–2316.
[9] Q.S. Mei, L. Zhang, K. Tsuchiya, H. Gao, T. Ohmura, K. Tsuzaki, Scripta Mater. 63 (2010) 977–980.
[10] L. Qian, X. Xiao, Q. Sun, T. Yu, Appl. Phys. Lett. 84 (2004) 1076–1078.
[11] T. Suzuki, M. Shimono, M. Wuttig, Scripta Mater. 44 (2001) 1979–1982.
[12] V.G. Pushin, V.V. Stolyarov, R.Z. Valiev, N.I. Kourov, N.N. Kuranova, E.A. Prokofiev, L.I. Yurchenko, Ann. Chim. Sci. Mat. 27 (2002) 77–88.
[13] K. Morsi, S. Goyal, J. Alloys Compd. 429 (2007) L1–L4.
[14] G. Purcek, O. Saray, O. Kul, I. Karaman, G.G. Yapici, M. Haouaoui, H.J. Maier, Mater. Sci. Eng. A 517 (2009) 97–104.
[15] T. Niendorf, D. Canadinc, H.J. Maier, I. Karaman, Scripta Mater. 60 (2009) 344–347.
[16] Y.J. Chen, Y.J. Li, J.C. Walmsley, S. Dumoulin, P.C. Skaret, H.J. Roven, Mater. Sci. Eng. A 527 (2010) 789–796.
[17] S. Luo, Q. Chen, Z. Zhao, J. Alloys Compd. 477 (2009) 602–607.
[18] S. Biswas, S.S. Dhinwal, S. Suwas, Acta Mater. 58 (2010) 3247–3261.
[19] W.N. Tang, R.S. Chen, E.H. Han, J. Alloys Compd. 477 (2009) 636–643.
[20] Q. Chen, S. Luo, Z. Zhao, J. Alloys Compd. 477 (2009) 726–731.
[21] Y. Huang, J.D. Robson, P.B. Prangnell, Acta Mater. 58 (2010) 1643–1657.
[22] S. Poortmans, L. Duchêne, A.M. Habraken, B. Verlinden, Acta Mater. 57 (2009) 1821–1830.
[23] H. Conrad, K. Jung, Scripta Mater. 53 (2005) 581–584.
[24] F.H.D. Torre, E.V. Pereloma, C.H.J. Davies, Acta Mater. 54 (2006) 1135–1146.
[25] T. Grosdidier, D. Goran, G. Ji, N. Llorca, J. Alloys Compd. 504 (2010) S456–S459.
[26] A. Hasani, L.S. Tóth, Scripta Mater. 61 (2009) 24–27.
[27] N. Tabatabaei, A.K. Taheri, M. Vaseghi, J. Alloys Compd. 502 (2010) 59–62.
[28] O.V. Mishin, J.R. Bowen, S. Lathabai, Scripta Mater. 63 (2010) 20–23.
[29] G.B. Hamu, D. Eliezer, L. Wagner, J. Alloys Compd. 468 (2009) 222–229.
[30] R. Lahoz, J.A. Puértolas, J. Alloys Compd. 381 (2004) 130–136.
[31] X. Xu, X. Lin, M. Yang, J. Chen, W. Huang, J. Alloys Compd. 480 (2009) 782–787.
[32] W. Tang, B. Sundman, R. Sandström, C. Qiu, Acta Mater. 47 (1999) 3457–3468.
[33] Z. Li, X. Cheng, Q. ShangGuan, Mater. Lett. 59 (2005) 705–709.
[34] Z. Li, G. Xiang, X. Cheng, Mater. Des. 27 (2006) 324–328.
[35] T. Waitz, T. Antretter, F.D. Fischer, N.K. Simha, H.P. Karnthaler, J. Mech. Phys. Solids 55 (2007) 419–444.
[36] S.N. Mathaudhu, K.T. Hartwig, Mater. Sci. Eng. A 426 (2006) 128–142.
[37] J.I. Kim, Y. Liu, S. Miyazaki, Acta Mater. 52 (2004) 487–499.
[38] T. Waitz, V. Kazykhanov, H.P. Karnthaler, Acta Mater. 52 (2004) 137–147.
[39] H. Matsumoto, Mater. Lett. 11 (1991) 40–42.
[40] M. Nishida, C.M. Wayman, T. Honma, Metall. Trans. 17A (1986) 1505–1515.
[41] V.I. Zel'dovich, G.A. Sobyanina, V.G. Pushin, Scripta Mater. 37 (1997) 79–84.
[42] T.H. Nam, T. Saburi, Y. Kawamura, K. Shimizu, Mater. Trans., JIM 31 (1990) 262–269.
[43] V.G. Pushin, V.V. Stolyarov, R.Z. Valiev, N.I. Kourov, N.N. Kuranova, E.A. Prokofiev, L.I. Yurchenko, Ann. Chim. Sci. Mater. 27 (2002) 77–88.
[44] I. Karaman, H.E. Karaca, Z.P. Luo, H.J. Maier, Metall. Mater. Trans. A 34 (2003) 2527–2539.
[45] A. Korbel, W. Bochniak, Scripta Mater. 51 (2004) 755–759.